Computing, Telecommunication and Control, 2023, Vol. 16, No. 4, Pp. 28–36.
Информатика, телекоммуникации и управление. 2023. Том 16, № 4. С. 28–36.

Simulations of Computer, Telecommunications, Control and Social Systems

Моделирование вычислительных, телекоммуникационных, управляющих и социально-экономических систем

Research article
DOI: https://doi.org/10.18721/JCSTCS.16403
UDC 621.36

CONTACT RESISTANCES INFLUENCE ON FLEXIBLE THERMOELECTRIC GENERATOR OUTPUT POWER

V.V. Loboda ✉

Peter the Great St. Petersburg Polytechnic University,
St. Petersburg, Russian Federation

✉ vera_loboda@mail.ru

Abstract. The calculation results of the influence of contact resistances of the metal-semiconductor interface on the output power of a flexible microthermoelectric generator is presented. The calculation method based on semiconductor theory. The contact area of the conductor (metal) and thermoelectric material (semiconductor) is characterized by a discrepancy between bulk properties and irregularities in a thin area near the interface. Different thermal and electrical carriers (phonons and electrons) encounter different resistances in this interface area. The calculations were carried out using ANSYS Workbench and Wolfram Mathematica. Output power simulation was carried out by taking into account contact electric and thermal resistances influence on the metal–semiconductor interface for six contact couples (three metals, two semiconductors). Interface contact resistances significantly reduce the output power. It was shown that contact resistances reduce the output power of the thermoelectric device by 64–70% depending on the metal type of the metal–semiconductor contact couple. The presented results of calculating interface contact resistances correspond to experimental measurements in references, which allows us to conclude that this method of calculating interface electrical and thermal contact resistances can be used in the case of microelectronic fabrication of thermoelectric devices.

Keywords: thermoelectric generator, contact resistances, simulation, ANSYS, output power

Aknolegement: This work was funded by State Assignment for Basic Research (project FSEG-2023-0016).

Citation: Loboda V.V. Contact resistances influence on flexible thermoelectric generator output power. Computing, Telecommunications and Control, 2023, Vol. 16, No. 4, Pp. 28–36. DOI: 10.18721/JCSTCS.16403

Научная статья
DOI: https://doi.org/10.18721/JCSTCS.16403
УДК 004.67

ВЛИЯНИЕ КОНТАКТНЫХ СОПРОТИВЛЕНИЙ НА ВЫХОДНУЮ МОЩНОСТЬ ГИБКОГО ТЕРМОЭЛЕКТРИЧЕСКОГО ГЕНЕРАТОРА

В.В. Лобода ✉

Санкт-Петербургский политехнический университет Петра Великого,
Санкт-Петербург, Российская Федерация

✉ vera_loboda@mail.ru

Аннотация. Представлены результаты расчета влияния контактных сопротивлений на границе раздела металл-полупроводник на выходную мощность гибкого микротермоэлектрического генератора. Метод расчета основан на теории полупроводников. Область контакта проводника (металла) и термоэлектрического материала (полупроводника) характеризуется несоответствием объемных свойств и неоднородностями в тонкой области вблизи границы раздела. Различные тепловые и электрические носители (фононы и электроны) будут встречать разное сопротивление в этой области интерфейса. Расчеты проводились с использованием программного обеспечения ANSYS Workbench и Wolfram Mathematica. Моделирование выходной мощности проведено с учетом влияния контактных электрических и термических сопротивлений на границу раздела металл-полупроводник для шести контактных пар (три металла, два полупроводника). Контактные сопротивления интерфейса существенно снижают выходную мощность. Показано, что контактные сопротивления снижают выходную мощность термоэлектрического устройства на 64–70% в зависимости от типа металла контактной пары «металл-полупроводник». Представленные результаты расчета интерфейсных контактных сопротивлений соответствуют экспериментальным измерениям в литературе, что позволяет сделать вывод о возможности использования данного метода расчета интерфейсных электрических и тепловых контактных сопротивлений при микроэлектронном изготовлении термоэлектрических устройств.

Ключевые слова: термоэлектрический генератор, контактные сопротивления, моделирование, ANSYS, выходная мощность

Финансирование: Работа выполнена в рамках Государственного задания на проведение фундаментальных исследований (код темы FSEG-2023-0016).

Для цитирования: Loboda V.V. Contact resistances influence on flexible thermoelectric generator output power // Computing, Telecommunications and Control. 2023. Т. 16, № 4. С. 28–36. DOI: 10.18721/JCSTCS.16403

Introduction

There are numerous power sources for low power consumption applications, but there exists a need to design improved alternative sources, and provide reliable and stable power supplies for microelectronic devices such as wireless sensor networks, smart homes, objects monitoring and mobile devices [1, 2]. Lately, the majority of research study on thermoelectric generators (TEG) has focused on volume and thin-film devices based on inorganic thermoelectric materials [3, 4]. One of the most promising types of TEGs that combine properties of inorganic thin-film semiconductor materials and an organic base is flexible microthermoelectric generators [5–7]. Thermoelectric devices design requires considering numerous factors related to the combination of different materials, the main of which are electric and thermal contact resistances. A great amount of research focuses on the influence of resistances on the metal–semiconductor interface [7–16]. Theoretical and experimental methods to measure resistances values are used. The values from the references range for electric contact resistances 10^{-14}–10^{-7} Ohm·m^2

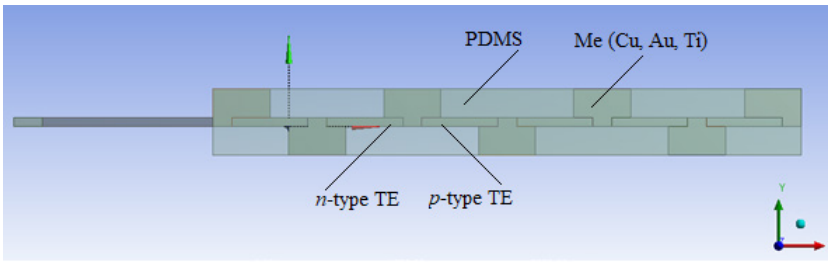

Fig. 1. 3D geometric model of Y-structure microthermoelectric generator

for thermal contact resistances: 10^{-10}–10^{-6} K / (W / m^2). It may be concluded from the references analysis results that application of this or that calculation method or measurements of contact resistances depends directly on semiconductor materials synthesis technology and device design.

The research goal is calculating contact resistance on the metal–semiconductor interface and determining their influence on output characteristics of a flexible microthermoelectric generator.

Contact resistances calculation method

A flexible Y-structure microthermoelectric generator was chosen as the object of the study [17, 18]. It consists of twenty-four *n*- and *p*-type thermoelements (TE) based on solid solutions Bi_2Te_3 and Sb_2Te_3 with contact conductors located between them. Fig. 1 shows a geometric 3D model of a flexible micro TEG. The TE have dimensions of 800 mm × 600 mm × 100 mm, metal contact connections are 600 mm × 600 mm × 300 mm. The rest of the TEG area is filled with a flexible substrate. Linear polymer polydimethylsiloxane (PDMS) is used as the flexible base. The total surface area of the device (S) was 26 mm^2.

The total internal electrical resistance of the TEG can be represented as the sum of series-connected resistors:

$$R_{\text{int}} = \sum_{i=1}^{2N} R_{\text{me}} + R_{\text{cont}},$$

where $R_{(n,\,p)}$ – TE resistance; R_{me} – resistance of metal; R_{cont} – contact resistance on the metal–semiconductor interface.

The internal resistance of the generator and, therefore, the maximum output power depends on the volume of the contact resistance [19].

The contact area of the conductor (metal) and thermoelectric material (semiconductor) is characterized by a discrepancy between bulk properties and irregularities in a thin area near the interface. Different thermal and electrical carriers (phonons and electrons) encounter different resistances in this interface area, resulting in lower power output from the device. The total thermal interface resistance is a circuit of parallel-connected resistances $(A_kR_k)_b$ is defined as [8]:

$$\frac{1}{(A_kR_k)_b} = \frac{1}{(A_kR_k)_{b,pp}} + \frac{1}{(A_kR_k)_{b,ee}} + \frac{1}{(A_kR_k)_{b,ep}} + \frac{1}{(A_kR_k)_{b,pe}}, \quad (1)$$

where A_k – TE cross-section area; R_k – thermal resistance; $(A_kR_k)_{b,pp}$ – phonon resistance; $(A_kR_k)_{b,ee}$ – electron resistance; $(A_kR_k)_{b,ep}$, $(A_kR_k)_{b,pe}$ – electron-phonon resistance. It is assumed that there is no direct heat transfer between the electron and phonon subsystems through the interface.

To calculate the phonon resistances, the diffuse mismatch model [8] is used, in which it is assumed that all phonons falling on the interface scatter.

The phonons boundary resistance may be calculated by the equation:

$$\frac{1}{\left(A_{\mathrm{k}}R_{\mathrm{k}}\right)_{\mathrm{b,pp}}}=\frac{T_{\mathrm{te}}-T_{\mathrm{mc}}}{q}, \tag{2}$$

where q – heat flux caused by an increase in the semiconductor temperature T_{te} relative to the substrate temperature T_{mc}.

The expression for the heat flux as a function of the phonon density of states may be represented starting from the general expression for the energy transferred per unit time from the semiconductor to the metal. Assuming that the transfer coefficient does not depend on the temperature on either side of the interface (only one side of the interface is considered):

$$q=\frac{h_{\mathrm{P}}\tau_{\mathrm{te}\to\mathrm{mc}}}{8\pi}\sum\nolimits_j U_{p(\mathrm{te},j)}\int_0^{\infty}P_{p,D}\left(\omega_p\right)\omega_p\left[\frac{1}{\exp\left(\dfrac{h_{\mathrm{P}}\omega_p}{2\pi k_{\mathrm{B}}T_{\mathrm{te}}}\right)}-\frac{1}{\exp\left(\dfrac{h_{\mathrm{P}}\omega_p}{2\pi k_{\mathrm{B}}T_{\mathrm{mc}}}\right)}\right]d\omega_p, \tag{3}$$

where h_{P} – Planck's constant; $\tau_{\mathrm{te}\to\mathrm{mc}}$ – heat transfer coefficient; $U_{p(\mathrm{te},j)}$ – the velocities of phonon modes in a semiconductor; $P_{p,D}$ – phonon states density; ω_p – angular frequency; k_{B} – Boltzmann's constant.

The phonon wave velocities (two transverse and one longitudinal) are calculated by the equation:

$$\sum\nolimits_j\frac{1}{U_{p(\mathrm{te},j)}}=\frac{1}{U_{p(\mathrm{te},l)}}+\frac{1}{U_{p(\mathrm{te},t)}}. \tag{4}$$

The transmission coefficient is approximated by the equation:

$$\tau_{\mathrm{te}\to\mathrm{mc}}=\frac{\sum_j u_{p(\mathrm{mc},j)}^{-2}}{\sum_j u_{p(\mathrm{te},j)}^{-2}+u_{p(\mathrm{mc},j)}^{-2}}. \tag{5}$$

Equation (5) is derived for the case when T_{te} equals T_{mc}, i.e. the equation gives a sufficient prediction of the transmission coefficient for a small $T_{\mathrm{te}}-T_{\mathrm{mc}}$. Usually, this temperature difference is about 1 K, which will be used in calculations.

The phonon velocity and Debye temperature are related to the Debye angular frequency ω_{D} through the equations:

$$\omega_{\mathrm{D}}=\left(6\pi^2u_p^3n\right)^{\frac{1}{3}}, \tag{6}$$

$$T_{\mathrm{D}}=\frac{h_{\mathrm{P}}\omega_{\mathrm{D}}}{2\pi k_{\mathrm{B}}}, \tag{7}$$

where n – the ratio of the number of primitive cells to the volume of a unit cell. Bi_2Te_3 and Sb_2Te_3 have non-primitive hexagonal unit cells three times the volume of a primitive rhombohedral cell [1].

The Debye density of phonon states is defined as:

$$P_{p,D}=\frac{\omega_p^2}{2\pi^2u_p^3}, \tag{8}$$

The boundary resistance of electrons was determined by the equation:

$$\frac{1}{\left(A_{\mathrm{k}}R_{\mathrm{k}}\right)_{\mathrm{b,ee}}}=\frac{\pi^2}{3}\frac{T}{\left(A_{\mathrm{k}}R_{\mathrm{e}}\right)_{\mathrm{b}}}\left(\frac{k_{\mathrm{B}}}{e_c}\right)^2, \tag{9}$$

where $(A_{\mathrm{k}}R_{\mathrm{e}})_{\mathrm{b}}$ – electrical interface resistance:

$$\frac{1}{\left(A_{\mathrm{k}}R_{\mathrm{e}}\right)_{\mathrm{b}}}=\frac{4\pi e^2 m_{\mathrm{e,te}}P}{h_P^3}\left[\frac{h_P^2E_0}{8\pi^2 m_{\mathrm{e,te}}d^2}\right]^{\frac{1}{2}}, \tag{10}$$

where $m_{\mathrm{e,te}}$ – effective mass of electrons/holes in thermoelectric material; e – electron charge; P – tunneling probability; E_0 – potential barrier height, d – potential barrier thickness.

The electrical contact resistance is calculated by the equation:

$$R_{\mathrm{e,c}}=\frac{4N_{\mathrm{te}}\left(A_{\mathrm{k}}R_{\mathrm{e}}\right)_{\mathrm{c}}}{A_{\mathrm{k}}}, \tag{11}$$

where N_{te} – number of thermoelements.

Table 1 displays the numerical values of the parameters of thermoelectric materials for calculating the thermal contact resistance.

Table 1

The parameters of thermoelectric materials [8]

Parameter	**Bi_2Te_3**	**Sb_2Te_3**
n, m^{-3}	$5.95\cdot10^{27}$	$6.40\cdot10^{27}$
ω_D, $rad\cdot s^{-1}$	$2.16\cdot10^{13}$	$2.09\cdot10^{13}$
u_p, $m\cdot s^{-1}$	3.058	2.888
$\tau_{\mathrm{te}\rightarrow\mathrm{mc}}$	0.56	0.54
τ_m, s	$2.5\cdot10^{-14}$	$9.8\cdot10^{-14}$
τ_e, s	$1.0\cdot10^{-11}$	$2.7\cdot10^{-11}$
$m_{\mathrm{e,te}}$	$0.58m_{\mathrm{e,o}}$	$1m_{\mathrm{e,o}}$
E_0, eV	0.15	0.2
d, nm	2.06	2.12

The calculation of contact resistances according to formulas (1–11) was carried out in the Wolfram Mathematica package, the results of calculations at T_{te} = 300 K are presented in Table 2. The solution of the problem of determining the influence of the contact resistance on the flexible micro TEG output power was carried out based on the finite element method using the ANSYS Workbench software platform. The simulation process consists of the following stages as indicated in Fig. 2.

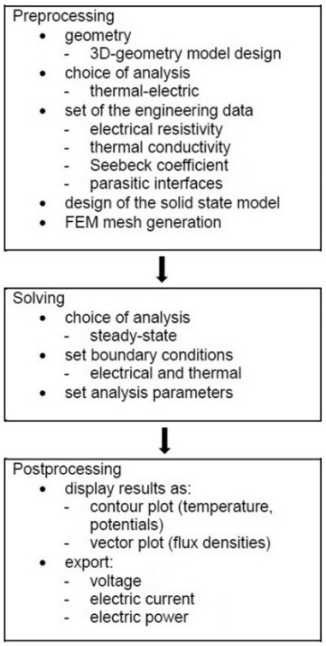

Fig. 2. Simulation process flow-chat

Table 2

Contact resistances calculation results

Thermal interface resistance	**Bi_2Te_3/Metal, K/(W/m²)**	**Sb_2Te_3/Metal, K/(W/m²)**
Phonon, Eq. (2),	$8.7\cdot10^{-8}$	$7.6\cdot10^{-11}$
Electron, Eq. (9)	$3.5\cdot10^{-7}$	$9.7\cdot10^{-7}$
Total, Eq. (1)	$6.9\cdot10^{-8}$	$7.0\cdot10^{-8}$
Electric interface resistance	Bi_2Te_3/Metal, (Ohm·m²)	Sb_2Te_3/Metal, (Ohm·m²)
Cu	$1.8\cdot10^{-8}$	$1.9\cdot10^{-8}$
Au	$2.3\cdot10^{-8}$	$2.5\cdot10^{-8}$
Ti	$3.3\cdot10^{-8}$	$4.1\cdot10^{-8}$

Preprocessing, Solving, Postprocessing. The Preprocessing stage includes five steps: 3-dimensional (3D) model design, choice of the thermal-electric analysis, setting of the engineering data that are physical parameters of materials and their interfaces, design of the solid state model of the thermoelectric generator using ANSYS Mechanical module, and generation of the finite-element mesh by ANSYS Meshing. The Solving stage includes three steps: choice of the steady-state analysis and its options, choice of the electrical and thermal initial conditions, choice of the analysis parameters. The load resistor R_L is modeled using additional APDL (ANSYS Parametric Design Language) procedure. The last stage deals with the output of calculated and simulated results in tables and figures. The simulation procedure is described in detail in [19–22].

Simulation Results

We simulated the output parameters of a flexible microthermoelectric generator for three different contact metals (Cu, Au, Ti) with and without taking into account contact resistances influence.

Bismuth and antimony tellurides of *n*-type and *p*-type conductivity were used as materials for micro-TEG thermoelements, as they provide the maximum thermoelectric efficiency in the considered temperature range. Initial data for simulation include the following physical parameters: Seebeck coefficient, electrical resistivity, thermal conductivity. These parameters largely depend on the semiconductor synthesis technology and have a significant spread. In this concern, the results of processing these parameters by the least-squares method [23] were used as the initial data. Physical parameters of substrate and metal were selected from the ANSYS library. The values of the physical parameters of the components materials of the TEG were used in the simulation for the temperature range of 300–400 K.

The temperature boundary conditions were determined by the temperature of the lower plate T_h and the temperature of the upper plate T_c. We considered the following temperatures: T_h = 318 K, 310 K, 303 K, T_c = 283 K, 280 K, 278 K. These temperatures correspond to the temperature difference between the hot and cold sides ΔT = 25 K, 30 K and 35 K, respectively. As electrical boundary condition, one of the load ports was set to ground (i.e. zero potential).

The results of the simulation are the values of the TEG output power at an external load and the specific power (power on the square unit). The values of the load resistance R_L varied from 0.5 to 30 Ohm. The output voltage was simulated at the load, while the output electric current and power were calculated. The maximum electric output power was calculated assuming that the load resistance was equal to the internal resistance of the generator, i.e. under the condition of transferring maximum electrical power to the load.

The simulation was carried out with and without taking into account the previously calculated contact resistances. The calculation results are presented in Table 3.

Table 3

The maximum output power and specific power of the TEG for various metals

Metal	without contact resistances influence		with contact resistances influence		Δ, %
	P_{max}, μW	P_{max}/S, μW/mm²	P_{max}, μW	P_{max}/S, μW/mm²	
ΔT = 25 K					
Cu	53.8	2.07	19.3	0.74	64
Au	53.8	2.07	19.2	0.74	64
Ti	53.8	2.07	16.3	0.63	70
ΔT = 30 K					
Cu	85.8	3.30	30.3	1.16	65
Au	85.8	3.30	30.2	1.16	65
Ti	85.8	3.30	25.5	0.98	70
ΔT = 35 K					
Cu	133.1	5.12	48.2	1.85	64
Au	133.1	5.12	48.1	1.85	64
Ti	133.1	5.12	40.8	1.57	69

The following results were achieved:

• contact electric and thermal resistances quite strongly influence the output characteristics of the microthermolectric devices, and reduce the output power of a device by 64–70% depending on the metal type of the metal–semiconductor contact couple;

• the greatest contribution to the decrease in output power is produced by the electrical contact resistance at the metal–semiconductor interface;

• the value of electric contact resistance increases in the order of Cu, Au and Ti;

• the value of the thermal contact resistance depends on the type of thermoelectric semiconductor material and does not depend on the choice of the metal of the contact couple.

Conclusions

The presented results of calculating interface contact resistances correspond to experimental measurements [12, 15], which allows us to conclude that this method of calculating interface electrical and thermal contact resistances can be used in the case of microelectronic fabrication of thermoelectric devices. We carried out an output power simulation by taking into account contact electric and thermal resistances influence on the metal–semiconductor interface for six contact couples (three metals, two semiconductors). Interface contact resistances significantly reduce the output power. The presented calculated method makes it possible not only to determine the optimal contact pairs, but also the value of the internal resistance, which in turn makes it possible to develop microelectronic thermoelectric devices, taking into account the operating conditions for power consumption with known external loads.

REFERENCES

1. **Champier D.** Thermoelectric generators: A review of applications, Energy Conversion and Management, 2017, Vol. 140, Pp. 167–181. DOI: 10.1016/J.ENCONMAN.2017.02.070

2. **Rodriguez R., Preindl M., Cotton J.S., Emadi A.** "Review and Trends of Thermoelectric Generator Heat Recovery in Automotive Applications," IEEE Trans. Vehicular Tech., 2019, Vol. 68, No. 6, Pp. 5366–5378. DOI: 10.1109/TVT.2019.2908150

3. **Yan J., Liao X., Yan D., Chen Y.** Review of Micro Thermoelectric Generator, J. Microelectromechanical Syst., 2018, Vol. 27, No. 1, Pp. 1–18. DOI: 10.1109/JMEMS.2017.2782748

4. **Pourkiaei S.M. et. al.** Thermoelectric cooler and thermoelectric generator devices: A review of present and potential applications, modeling and materials, Energy, 2019, Vol. 186, No. 115849, Pp. 1–17. DOI: 10.1016/J.ENERGY.2019.07.179

5. **Deng F., Qiu H., Chen J., Wang L., Wang B.** Wearable Thermoelectric Power Generators Combined With Flexible Supercapacitor for Low-Power Human Diagnosis Devices, IEEE Transactions on Industrial Electronics, 2017, Vol. 64, No. 2, Pp. 1477–1485. DOI: 10.1109/TIE.2016.2613063

6. **Du Y., Xu J., Paul B., Eklund P.** Flexible thermoelectric materials and devices, J. Applied Materials Today, 2018, Vol. 12, Pp. 366–388. DOI: 10.1016/J.APMT.2018.07.004

7. **Wang Y. et al.** Flexible Thermoelectric Materials and Generators: Challenges and Innovations, J. Advanced Materials, 2019, Vol. 31, Pp. 1807916. DOI: 10.1002/adma.201807916

8. **Da Silva L.W., Kaviany M.** Micro-thermoelectric cooler: interfacial effects on thermal and electrical transport, J. International Journal of Heat and Mass Transfer, 2004, Vol. 47, Pp. 2417–2435. DOI: 10.1016/J.IJHEATMASSTRANSFER.2003.11.024

9. **Kim C.H.** Development of a numerical method for the performance analysis of thermoelectric generators with thermal and electric contact resistance, J. Applied Thermal Engineering, 2018, Vol. 108, Pp. 408–417. DOI: 10.1016/j.applthermaleng.2017.10.158

10. **Chen B. et al.** Flexible thermoelectric generators with inkjet-printed bismuth telluride nan-owires and liquid metal contacts, Nanoscale, 2019, Vol. 11, Pp. 5222–5230. DOI: 10.1039/c8nr09101c

11. **Luo Y., Kim C.H.** Effects of the cross-sectional area ratios and contact resistance on the performance of a cascaded thermoelectric generator, J. International Journal of Energy Research, 2019, Vol. 43, No. 3, Pp. 572–596. DOI: 10.1002/ER.4426

12. **Lahmar A. et al.** Experimental investigation on the thermal contact resistance between gold coating and ceramic substrates, J. Thin Solid Film, 2001, Vol. 389, Pp. 167–172. DOI: 10.1016/S0040-6090(01)00774-X

13. **Sim M., Park H., Kim S.** Modeling and Extraction of Parasitic Thermal Conductance and Intrinsic Model Parameters of Thermoelectric Modules, J. Journal of Electronic Materials, 2015, Vol. 44. No. 11, Pp. 4473–4481. DOI: 10.1007/s11664-015-3985-0

14. **Gao Y. et al.** Nanostructured Interfaces for Thermoelectrics, J. Journal of Electronic Materials, 2010, Vol. 39, Pp. 1456–1462. DOI: 10.1007/S11664-010-1256-7

15. **Gupta R.P., Mccarty R., Sharp J.** Practical Contact Resistance Measurement Method for Bulk Bi2Te3-Based Thermoelectric Devices, J. Journal of Electronic Materials, 2014, Vol. 43, No. 6, Pp. 1608–1612. DOI: 10.1007/s11664-013-2806-6

16. **Hodes M.** Optimal Design of Thermoelectric Refrigerators Embedded in a Thermal Resistance Network, J. IEEE Transactions on Components, Packaging and Manufacturing Technology, 2012, Vol. 2, No. 3, Pp. 483–495. DOI: 10.1109/TCPMT.2011.2166762

17. **Nguyen H.T., Nguyen V.T., Takahito O.** Flexible thermoelectric power generator with Y-type structure using electrochemical deposition process, Applied Energy, 2018, Vol. 210, Pp. 467–476. DOI: 10.1016/J.APENERGY.2017.05.005

18. **Buslaev R., Galitskaya A., Loboda V.** Simulation of Flexible Thermoelectric Generators Based on Bi2Te3/Sb2Te3 Synthesized by Electrochemical Deposition Method, in Proc. IEEE International Conference on Electrical Engineering and Photonics (EExPolytech), 2019, Pp. 54–57.

19. **Korotkov A.S., Loboda V.V.** Thermoelectricity: From History to Modernity through the CASS Activity, IEEE Circuits and Systems Magazine, 2021, Vol. 21, No. 3, Pp. 57–65. DOI: 10.1109/mcas.2021.3092534

20. **Loboda V., Buslaev R.** Optimization Calculation of Thermoelement Linear Dimensions for Microthermoelectric Generator, in Proc. 2020 IEEE East-West Design & Test Symposium (EWDTS), Varna, Bulgaria, 4–7 September 2020. DOI: 10.31114/2078-7707-2020-3-230-236

21. **Buslaev R., Loboda V.** Simulation of Uni-leg Thermoelectric Generator, in Proc. IEEE International Conference on Electrical Engineering and Photonics, (EExPolytech), 2018, Pp. 27–31. DOI: 10.1109/EEXPOLYTECH.2018.8564405

22. **Korotkov A.S., Loboda V.V.** Simulation and Design of Thin-Film Thermoelectric Generators, in Proc. International Symposium on Fundamentals of Electrical Engineering (ISFEE), Bucharest, Romania, 4 pages, 1–3 November, 2018. DOI: 10.1109/ISFEE.2018.8742452

23. **Korotkov A.S., Loboda V.V., Dzyubanenko S.V., Bakulin E.M.** Design of a Thin-Film Thermoelectric Generator for Low-Power Applications, Russian Microelectronics, 2019, Vol. 48, No. 5, Pp. 326–334. DOI: 10.1134/s1063739719040061

INFORMATION ABOUT AUTHOR / СВЕДЕНИЯ ОБ АВТОРЕ

Loboda Vera V.
Лобода Вера Владимировна
E-mail: vera_loboda@mail.ru
ORCID: https://orcid.org/0000-0003-3103-7060

Submitted: 16.11.2023; Approved: 13.12.2023; Accepted: 21.12.2023.
Поступила: 16.11.2023; Одобрена: 13.12.2023; Принята: 21.12.2023.